HHS Public Access

A novel gene editing system to treat both Tay-Sachs and Sandhoff diseases

Li Ou[1], **Michael J Przybilla**[2], **Alexandru-Flaviu Tăbăran**[3], **Paula Overn**[3], **M. Gerard O'Sullivan**[3], **Xuntian Jiang**[4], **Rohini Sidhu**[4], **Pamela J. Kell**[4], **Daniel S. Ory**[4], **Chester B. Whitley**[1,2]

[1]Gene Therapy Center, Department of Pediatrics, University of Minnesota, Minneapolis, MN 55455

[2]Department of Genetics, Cell Biology and Development, University of Minnesota, Minneapolis, MN 55455

[3]Comparative Pathology Shared Resource, University of Minnesota Masonic Cancer Center, Saint Paul, MN 55108

[4]Department of Medicine, Washington University School of Medicine, Saint Louis, Missouri

Abstract

The GM2-gangliosidoses are neurological diseases causing premature death, thus developing effective treatment protocols is urgent. GM2-gangliosidoses result from deficiency of a lysosomal enzyme β-hexosaminidase (Hex) and subsequent accumulation of GM2 gangliosides. Genetic changes in HEXA, encoding the Hex α subunit, or HEXB, encoding the Hex β subunit, causes Tay-Sachs disease and Sandhoff disease, respectively. Previous studies have showed that a modified human Hex μ subunit (HEXM) can treat both Tay-Sachs and Sandhoff diseases by forming a homodimer to degrade GM2 gangliosides. To this end, we applied this HEXM subunit in our PS813 gene editing system to treat neonatal Sandhoff mice. Through AAV delivery of the CRISPR system, a promoterless HEXM cDNA will be integrated into the albumin safe harbor locus, and lysosomal enzyme will be expressed and secreted from edited hepatocytes. Four months after the i.v. of AAV vectors, plasma MUGS and MUG activities reached up to 144- and 17-fold of wildtype levels (n=10, p<0.0001), respectively. More importantly, MUGS and MUG activities in the brain also increased significantly compared with untreated Sandhoff mice (p<0.001). Further, HPLC-MS/MS analysis showed that GM2 gangliosides in multiple tissues, except the brain, of treated mice were reduced to normal levels. Rotarod analysis showed that coordination and motor memory of treated mice were improved (p<0.05). Histological analysis of H&E stained tissues showed reduced cellular vacuolation in the brain and liver of treated Sandhoff mice. These results

Corresponding author: Li Ou, PhD, Assistant Professor, Gene Therapy Center, University of Minnesota, 5-174 MCB, 420 Washington Ave SE, Minneapolis, MN 55455, ouxxx045@umn.edu, Phone: (612) 625-6912.

demonstrate the potential of developing a treatment of *in vivo* genome editing for Tay-Sachs and Sandhoff patients.

Keywords

Sandhoff disease; GM2-gangliosidosis; gene editing; safe harbor

1. INTRODUCTION

GM2-gangliosidoses, including Sandhoff disease and Tay-Sachs disease, are genetic disorders causing severe neurological diseases and premature death. GM2-gangliosidoses result from deficiency of a lysosomal enzyme β-hexosaminidase A and subsequent accumulation of GM2 gangliosides. Genetic changes in HEXA, encoding the Hex α subunit, or HEXB, encoding the Hex β subunit, causes Tay-Sachs and Sandhoff disease, respectively. Since the genotype-phenotype correlation is not well established in spite of many efforts using in silico tools [1–3], the diagnosis of GM2-gangliosidosis is often a long and burdensome odyssey. A recent natural history study of gangliosidoses mapped the timeline of clinical changes, which lays a solid foundation for developing therapies [4]. However, there is no effective treatment for GM2-gangliosidoses now, with palliative measures being the current standard of care. Even in a patient with the attenuated form, B1 variant of GM2-gangliosidosis [5], stem cell transplantation achieved increased enzyme activities but could not prevent the disease progression and demise. Gene therapy, a promising strategy, is being investigated in animal models. There have been attempts using AAV vectors to treat GM2-gangliosidoses in animal models [6–8] and one clinical trial (Axovant). However, major obstacles must still be overcome including: (1) continuous, rather than pulsatile, delivery; (2) sufficient transgene product to the brain; (3) minimizing the vector-associated risk. Therefore, there is a critical need to develop an innovative gene therapy protocol which surmounts these problems for treating GM2-gangliosidoses.

Preliminary results demonstrate that zinc finger nuclease (ZFN)-mediated *in vivo* genome editing successfully treats MPS I mice [9]. MPS I mice received i.v. administration of 3 different AAV vectors encoding ZFN (left and right arms) and promoterless IDUA cDNA. These AAV vectors efficiently facilitate insertion of IDUA sequence into the albumin locus. The endogenous albumin promoter drives IDUA transgene expression, treating other tissues through cross correction. More importantly, Barnes maze test and histological analysis showed that this liver-targeting gene therapy achieved significant neurological improvements. This study led to a Phase I clinical trial (ClinicalTrials.gov identifier: NCT02702115). Progress reports from this clinical trial showed no drug-related adverse events, but a low level of transgene expression [10]. As shown in clinical trials for treating Hemophilia B, a relatively low efficiency is also an obstacle for traditional AAV gene therapies. Increasing the dose will bring about higher risk of toxicity, more challenging vector production and increased manufacturing costs.

Thus, the present study aims to further improve the efficacy of gene editing by using the CRISPR system. Recently, a modified human Hex μ subunit (HEXM), incorporating

sequence of both α and β subunits by forming a homodimer to degrade GM2 gangliosides [6], has been shown to able to treat both Sandhoff and Tay-Sachs diseases [7,8]. Therefore, neonatal Sandhoff mice were injected with a dual AAV system (AAV8-SaCas9 and AAV8-HEXM-sgRNA), designated as PS813 (proprietary system 813). A series of analyses were performed to assess the treatment efficacy. This is the first attempt to apply *in vivo* gene editing to treat GM2-gangliosidoses.

2. MATERIALS AND METHODS

2.1 Animals and injections

Sandhoff mice (*Hexb–/–*), purchased from the Jackson Laboratory, were generated by inserting a neomycin resistance cassette into exon 13 of the *Hexb* gene on the 129S4/SvJae background [12]. Sandhoff mice (*Hexb–/–*) and control mice were genotyped by PCR. Neonatal mice were injected with AAV vectors (<30 μL) through temporal facial vein on postnatal Day 1 or 2. Hydrodynamic injections of plasmids were performed in adult Sandhoff mice as previously described [13]. All mouse care and handling procedures were in compliance with the rules of the Institutional Animal Care and Use Committee (IACUC) of the University of Minnesota.

2.2 Construct design and *in vitro* confirmation

Four guide RNAs (gRNAs) were designed based on the locations to the insertion site (albumin locus) and their off-target profiles. Then, these gRNAs were cloned into the pX602-AAV-TBG saCas9 plasmid. Each plasmid was transfected into mouse embryonic fibroblast (MEF) cells, and cells were subsequently harvested for PCR amplification. In order to determine the gRNA cleavage activity of the gRNA constructs, an *in vitro* Surveyor assay was performed on the PCR product (Surveyor mutation detection kit, Transgenomic, NE, USA, #706020).

2.3 Vector production

AAV-HEXM-gRNA and AAV-SaCas9 were packaged into AAV8 vectors at the Children's Hospital of Philadelphia Research Vector Core. The titer was verified by SDS PAGE and silver staining. The core follows Good Laboratory Practice (GLP) guidelines.

2.4 Depletion of brain capillaries

To rule out the possibility that enzyme activities in the brain come from capillary cells and blood, all mice were transcardially perfused with 35 mL PBS, and depletion of brain capillaries was performed as previously described [14].

2.5 Hex enzyme assay

Tissues were homogenized and protein concentrations were measured as previously described [15]. MUG and MUGS enzyme activities in plasma and tissues were measured using a previously described enzyme assay protocol [15]. 4-Methylumbelliferyl N-acetyl-b-D-glucosaminide (4MUG, Sigma, MO, USA, # M2133) and 4-Methylumbelliferyl-6-

sulfa-2-Acetoamido-2-Deoxy-beta-D-Glucopyranoside Potassium salt (4MUGS, TRC, Canada, # M335000) were used for measuring MUG and MUGS activities, respectively.

2.6 Ganglioside quantification

GM2 gangliosides were quantified using HPLC-MS/MS as previously described [16]. The mouse brain (1g wet tissue/6 mL CHAPS solution), heart (1g wet tissue/6 mL CHAPS solution), liver (1g wet tissue/6 mL CHAPS solution), and spleen (1g wet tissue/6 mL CHAPS solution) samples were homogenized in 2% CHAPS solution. Protein precipitation with 200 μL of methanol was conducted to extract GM2 gangliosides from 50 μL of tissue homogenates. d3-GM2(18:0) was used as internal standards. The quality control samples (10% study sample extracts from each tissue type) were used to monitor the instrument performances. Sample analysis was conducted with the Shimadzu 20AD HPLC system, coupled with the 6500QTRAP mass spectrometer operated in the positive MRM mode. Data processing was conducted with Analyst 1.5.2 (Applied Biosystems, CA, USA). The relative quantification of lipids was provided, and the data were reported as the peak area ratios of the analytes to the corresponding internal standards.

2.7 Behavior tests

The pole test was performed as previously described [17]. Rotarod analysis was performed using an adapted protocol previously described [18]. Fear conditioning was performed according to an established protocol [19]. All three behavior tests were performed at the Mouse Behavior Core, University of Minnesota.

2.8 Histology

After perfusion and fixation in 10% neutral buffered formalin, tissues from 9 mice (3/group) were processed into paraffin using standard histology techniques, sectioned at a thickness of 4 μm, stained with hematoxylin and eosin (H&E), and evaluated by ACVP-board certified pathologists (A-FT, MGO'S) using light microscopy. All work was done at the University of Minnesota Masonic Cancer Center Comparative Pathology Shared Resource Laboratory.

2.9 QPCR

Total DNA from brain, heart, liver, and spleen of treated and control mice was extracted with the QIAamp DNA Mini kit (QIAGEN, Germany). QPCR was performed with PowerUp SYBR Green Master Mix (Thermo Fisher, MA, USA) in MicroAmp 96-well plate (Applied Biosystems, CA, USA). Primers targeting the AAV ITR was as followed: Fwd primer, 5'-GGAACCCCTAGTGATGGAGTT-3'; Rev primer, 5'-CGGCCTCAGTGAGCGA-3'. Plasmids encoding the AAV ITR was used to make a standard curve. gDNA was quantified in parallel samples using GAPDH primers as internal controls. Fwd primer, 5'-CATCACTGCCACCCAGAAGACTG-3'; Rev primer, 5'-ATGCCAGTGAGCTTCCCGTTCAG-3'. AAV copy number was expressed as 100 vg/ng DNA.

2.10   Statistical analysis

Statistical analysis was performed with Graphpad Prism 7. One-way ANOVA for multiple comparisons, and two-sided t test for comparisons between two groups (adjusted for multiple comparisons). The results met the normal distribution assumptions. The variance between groups that are being compared was similar. Data were represented as Mean ± SEM. $*p<0.05$ when comparing treated to untreated Sandhoff mice, $**p<0.01$, $***p<0.001$, $****p<0.0001$. The sample size was determined through power analysis with pilot study results. The n number indicated biological replicates, while experiments were replicated in triplicate. No outliers were excluded. No randomization was performed. Group assignment was blinded to staff performing the behavior tests.

3.   RESULTS

3.1   Construct design and verification

The design for CRISPR-mediated genome editing is illustrated in Fig. 1A. SaCas9 and guide RNA mediate the insertion of promoterless cDNA donor into albumin locus and achieve expression of Hex enzyme. AAV8 vectors are liver-tropic, and SaCas9 is under control of a liver-specific promoter. By virtue of this, genome editing and transgene expression can be limited to hepatocytes. Systemic therapeutic benefits are expected to be achieved through a phenomenon called 'cross correction' [20]. A total of four guide RNAs (gRNAs) were transfected into mouse embryonic fibroblast cells together with SaCas9. The ability of these gRNAs to guide SaCas9-mediated cleavage at the albumin locus and to promote DNA double strand break was evaluated via the Surveyor assay. The results showed that one of the gRNAs mediated targeted DNA cleavage with the highest efficiency (11% indels) (Fig. 1B), and was selected for the following studies.

In addition, the plasmids encoding SaCas9 and HEXB cDNA donor were tested in adult Sandhoff mice through hydrodynamic injection. Only the mice receiving both plasmids had significant higher MUG activities in the liver (45% of wildtype levels, $p<0.05$, Fig. 1C). Notably, there is no significant increase in β-hexosaminidase S (αα) activities, indicating that the increase of MUG activities mainly comes from β-hexosaminidase B (ββ) through transgene expression of HEXB cDNA. Mice receiving the plasmid encoding promoterless cDNA donor showed no increase in MUG or MUGS activities. These results strongly support the feasibility of this CRISPR-mediated 'safe harbor' genome editing strategy in treating Sandhoff mice.

3.2   Proof-of-concept study with hydrodynamic injections

Since GM2-gangliosidoses are primarily neurological diseases, previous gene therapy studies focused on direct injection into the brain. One challenge for PS813 to treat a neurological disease is to deliver the enzyme to the brain. However, previous studies (summarized in Table 1) using high dose enzyme replacement therapy have achieved significant neurological benefits in MPS I mice [21], MPS II mice [22], MPS IIIA mice [23], MPS VII mice [24], Krabbe mice [25], metachromatic leukodystrophy mice [26], α-mannosidosis mice [27] and aspartylglycosaminuria mice [28]. These results indicated that when there is a constant high enzyme level in the bloodstream, a small amount may be able

to cross the BBB. In addition, our previous ZFN-mediated liver-targeting gene editing approach also achieved amelioration of neurological diseases in MPS I [9] and II mice [29].

To further support this, hydrodynamic injection of a plasmid encoding HEXM sequence into adult Sandhoff mice was performed. To eliminate any transgene expression in the CNS, the HEXM expression was restricted in the liver by using a liver-specific promoter/enhancer (the human α−1-antitrypsin [hAAT] promoter and human apolipoprotein [ApoE] enhancer). Two days after the injection, the mice were transcardially perfused, and depletion of brain capillaries was performed. Interestingly, a significant increase in MUGS and MUG activities were observed in the brain of injected mice (p<0.05, Fig. 2). These results indicated that Hex proteins were expressed in the liver, resulting in high blood Hex enzyme levels and a small, but sufficient, amount of Hex enzyme in the CNS. In addition, the fact that both MUGS and MUG activities increased support the therapeutic potential of the HEXM sequence in treating both Tay-Sachs and Sandhoff diseases.

3.3 AAV delivery of the gene editing system to treat Sandhoff mice

3.3.1 Hex enzyme activities—Neonatal Sandhoff mice (n=10) received co-delivery of AAV8-SaCas9 (5×10^9 vg/g body weight) and AAV8-HEXM-gRNA (3×10^{10} vg/g body weight) through temporal facial vein. A group of Sandhoff mice receiving the donor only (AAV8-HEXM-gRNA, n=4) was also included as controls. Plasma MUGS and MUG activities in Cas9+donor treated Sandhoff mice increased significantly up to 144 and 17 fold of wildtype levels, respectively (p<0.0001, Fig. 3A and B). In mice treated with the donor alone, the MUGS and MUG activities did not significantly increase (data not shown), indicating that there was no episomal transgene expression from the promoterless donor. After 4 months, all mice were euthanized and tissues were harvested for further analyses. MUGS activities in the liver, heart and spleen increased to 25, 3 and 2 fold of wildtype levels, respectively (p<0.0001, Fig. 3C). MUG activities in the liver, heart and spleen increased 7 fold, 120% and 79% of wildtype levels, respectively (Fig. 3D). More interestingly, MUGS and MUG activities in the brain of Cas9+donor treated mice also increased significantly (Fig. 3C and 3D, compared with untreated Sandhoff mice, p<0.001).

3.3.2 Behavior tests—Three months post dosing, a battery of behavior tests was performed to assess the treatment efficacy. In the pole test (assessing bradykinesia) and the fear conditioning (assessing learning and memory), no significant differences were observed between untreated Sandhoff mice and normal mice. A previous study showed that Sandhoff mice had indistinguishable performance from wildtype mice at the age of 6 weeks old and 3 months old in the fear conditioning [30]. These results indicate that at least at this age, these two tests could not distinguish Sandhoff mice from normal mice. However, in the rotarod test, which assesses coordination, motor function and motor memory, a significant difference between untreated Sandhoff and normal mice were observed. Moreover, the Cas9+donor treated mice had significantly improved performance compared with untreated Sandhoff mice (Fig.4, p<0.05). These results indicate that this liver-targeting gene therapy achieved neurological benefits.

3.3.3 Histopathology—Cellular vacuolation is the characteristic microscopic finding of lysosomes engorged with storage materials in the murine model of lysosomal diseases. To assess whether the treatment can reduce cellular vacuolation, histological analysis of the brain and liver was performed. Untreated Sandhoff mice showed the typical hepatic and cerebral lesions associated with lysosomal accumulation: Kupffer cell and neuronal cell hypertrophy and vacuolation (with small, well defined vesicles of variable sizes and with clear to pale-eosinophilic content, pointed by arrows and illustrated in the enlarged photo in the center panel) (Fig. 5). Moreover, within the brain, the lysosomal accumulation (manifested as cellular vacuolation) is present in variable degrees in all the main anatomic areas (brain cortex, hippocampus, thalamus, hypothalamus, pons and cerebellum). In contrast, there is an absence of Kupffer cell vacuolation in treated Sandhoff mice (n=3), with the morphology of the liver being comparable from this perspective to normal mice. Neuronal lysosomal accumulation was reduced in 1 of 3 treated Sandhoff mice. In addition, no evidence of vector-associated toxicity was observed through the H&E staining analysis, which supports the safety profile of PS813.

3.3.4 GM2 gangliosides—Further, HPLC-MS/MS was applied to quantify the GM2 gangliosides in tissues. As shown in Fig. 6, the amount of GM2 gangliosides in the brain is generally magnitude higher than that in other tissues. GM2 gangliosides were significantly reduced in the liver, heart and spleen of treated mice (p<0.0001). However, GM2 gangliosides in the brain of treated mice were not significantly reduced (Fig. 6D). Considering the fact that there is substantial amount of gangliosides in the membrane of neurons, one possible explanation is that a very small reduction (even not statistically significant) in the total amount of GM2 gangliosides may lead to reduced cellular vacuolation (Fig. 5) and therapeutic benefits.

3.3.5 Biodistribution of AAV vector—To determine the biostribution of AAV vectors, total DNA extracted from treated Sandhoff mice (n=6), untreated Sandhoff mice (n=4), and normal mice (n=4) was assayed by QPCR to quantify AAV copy number (data summarized in Table 2). No AAV vector was detected from tissues of control mice. The liver of treated Sandhoff mice has the highest copy number, followed by heart. Notably, the copy number in the spleen of treated mice was non-detectable. Previous studies have shown that AAV8 vector can cross the BBB [31]. Similarly, a small amount of AAV vector was observed in the brain. However, it is unlikely that gene editing occurred in the brain because Cas9 is under the control of a liver-specific promoter.

4. DISCUSSION

4.1 HEXM has the potential to treat both Tay-Sachs and Sandhoff disease

Although expressing only β subunit is expected to efficiently treat Sandhoff mice, the sialidase bypass does not exist in humans, making translation of this strategy into clinical practice difficult. Further, optimal production of Hex A enzyme is suggested to be expressing both subunits because the overexpression of one subunit may rapidly deplete the pool of its endogenous subunit partner [32]. As shown in Fig.1C, expression of the HEXB construct achieved increase in MUG activities, but not MUGS activity. In contrast,

expression of the HEXM construct achieved increase in both MUGS and MUG activities (Fig.2 & Fig.3). Previous study [33] also showed that co-expression of both subunits achieved higher Hex A activities in Sandhoff mice or cats. However, it is difficult to package both HEXA and HEXB cDNA into one AAV vector, while the use of two vectors brings about higher manufacturing cost and vector-associated risk. To this end, a modified α subunit incorporating partial sequence of β-subunit was designed [6]. This modified subunit (μ) can form a stable dimeric enzyme to efficiently degrades GM2 gangliosides. These results indicate that this homodimer can properly interact with the activator protein, which is required for the catalytic degradation of GM2 gangliosides [34]. Expression of HEXM is expected to achieve greater therapeutic benefits than that is achieved through expression of one subunit alone, which would result predominantly in the formation of either Hex S (αα) or Hex B (ββ). Another benefit for using this HEXM construct is the ability to treat both Tay-Sachs and Sandhoff diseases as shown in two studies [6,7]. In this study, application of the HEXM construct successfully achieved significant MUGS and MUG activities, demonstrating its remarkable therapeutic potential.

In addition, it will be interesting to assess the potential immune response against HexM proteins. However, this study was performed in neonatal mice that might be immune naïve and immunotolerized. Plasma enzyme activities were stable from day 30, to 60 and 90, indicating that immune response, if any, did not significantly affect the enzyme activities.

4.2 CRISPR-mediated gene editing to treat lysosomal diseases

There are no effective therapies for the GM2-gangliosidoses, with palliative measures being the current standard of care. Enzyme replacement therapy [35], substrate reduction therapy [36], chemical chaperone therapy [37] and bone marrow transplantation [38], only achieve limited therapeutic benefit in animal models. Gene therapy holds promise for treating lysosomal diseases as it has potential for permanent, single-dose treatment. GM2 animal model studies include gene modification using lentiviral [39] and AAV vectors [40], but these methods have integration and persistence drawbacks. Integrating vectors, such as lentiviral vectors, randomly integrate into the genome, raising potential concerns of insertional mutagenesis [41]. Clinical trials treating X-linked severe combined immunodeficiency with retroviral gene therapy resulted in leukemia for 2 patients through oncogene activation by vector integration. Meanwhile, AAV, mainly an episomal vector, is not expected to provide permanent transgene expression. It was shown that transgene expression from episomal AAV vectors was rapidly lost after one round of cell division [42], leading to a gradual decline of therapeutic effects. Unfortunately, secondary administration of AAV vectors often fails to rescue expression, due to the immune response to primary vector delivery [43]. Therefore, the major advantage of PS813 over traditional AAV gene therapy is its ability to create life-long enzyme replacement therapy, overcoming the issue of vector dilution, and will provide ongoing efficacy after the first few years following treatment.

In our previous study with ZFNs, the genome modification rate was relatively low. The low probability of all 3 AAV vectors transfecting the same cell explains this low efficiency modification rate. Progress reports from this clinical trial showed no drug-related adverse

events, but a low level of transgene expression [10]. As shown in clinical trials for treating Hemophilia B, a relatively low efficiency is also an obstacle for traditional AAV gene therapies. Increasing the dose will bring about higher risk of toxicity, more challenging vector production and increased manufacturing costs. Therefore, a PS813 gene editing system was designed utilizing Cas9. As opposed to 3 AAV vectors used in the study with ZFNs, this CRISPR system only requires 2 vectors: one AAV vector encoding SaCas9, the other encoding the promoterless donor sequence and guide RNA. Assuming similar doses, AAV transduction and nuclease targeting efficiency, the efficiency of successful genome editing by CRISPR is expected to be higher than that mediated by ZFNs. In the parallel study in MPS I mice, PS813 achieved a magnitude higher efficiency than that achieved by the ZFN system (unpublished data). As shown in this study, PS813 achieves increased enzyme level in the brain of Sandhoff mice at the dose of 3.5×10^{13} vg/kg (Fig. 3C&D). Meanwhile, previous studies in Sandhoff mice could not achieve increased enzyme level in the brain at the same dose (3.5×10^{13} vg/kg AAV9) [44], or even a higher dose (5×10^{13} vg/kg scAAV) [6]. In light of its remarkable efficiency, PS813 will bring a novel therapy with higher efficiency and reduced risk to patients with Tay-Sachs or Sandhoff disease.

In 2018, the FDA has approved an IND application based on Cas9 for treating Leber congenital amaurosis type 10 [45]. More recently, a study used a GOTI method (genome-wide off-target analysis by two-cell embryo injection) to determine off-target effects by editing a blastomere of two-cell mouse embryos using Cas9 [46]. This method separates off-target signals from background noise by using cells with the identical genetic background as controls. Comparison between the whole genome of progeny cells of edited vs non-edited blastomeres identified very rare off-target events (similar to spontaneous mutations). These facts support the safety and potential clinical application of CRISPR/Cas9.

4.3   Intravenous administration to treat neurological diseases

Although the pathophysiology is not fully understood [47], the GM2-gangliosidoses are primarily neurological disorders. Therefore, many previous gene therapy studies focused on direct injections into the brain. These approaches are of limited use due to several drawbacks: (1) highly invasive nature; (2) difficulty in achieving uniform and global distribution throughout the brain [48]; (3) the inability to treat systemic diseases that become prominent when animals live longer because neurological diseases are treated [41]; (4) genotoxicity due to overexpression of Hex A in neurons [49]. In addition, there have been attempts using intravenous administration of AAV-BR1 [50] and AAV9 vectors [44] to treat gangliosidosis. As discussed earlier, the drawback of traditional AAV gene therapy is vector dilution and gradual loss of therapeutic benefits. Alternatively, fusing lysosomal enzyme with other proteins to target the CNS has also been tested [51], while the application into gangliosidoses has not yet accomplished. The feasibility of this liver-targeting gene editing approach to treat a neurological disease is supported by multiple preclinical studies with high doses of ERT that are relatively high compared to usual doses of ERT used to treat patients with (Table 1). These studies showed that a high level of enzyme in circulation could facilitate entry of enzyme into the brain. This phenomenon was also observed in our previous ZFN studies in MPS I [9] and II [29]. Possible mechanisms may include: 1) impaired integrity of BBB due to disease; 2) fluid-phase pinocytosis; 3) extracellular

pathway; 4) residual mannose 6-phosphate receptor (M6PR) or other uncharacterized receptors. Admittedly, the fact that GM2 gangliosides levels were not significantly reduced in the brain seems confusing, However, rotarod analysis showed improvements in motor function of treated Sandhoff mice, and histological analysis showed reduced neuronal vacuolation. Although the treatment efficacy in the brain needs to be optimized, these results support that this liver-targeting gene therapy can achieve significant neurological benefits. Moreover, considering the dose used in this study is relatively low (3.5×10^{10} vg/g body weight), the treatment efficacy in the brain can be significantly improved by increasing the dose. It was possible that due to saturation of M6P-mediated lysosome-targeting pathway by overexpression of one lysosomal enzyme, other lysosomal enzymes might not be efficiently delivered to the lysosome. In our previous study, we found that IDS enzyme activity in cells expressing over 200-fold of wildtype IDUA levels were not significantly reduced [15]. Thus, overexpression of one lysosomal enzyme does not necessarily significantly affect expression of other lysosomal enzymes. IDUA enzyme activity in the liver of untreated Sandhoff, treated Sandhoff, and heterozygous normal mice were also measured. There was no significant difference between groups (data not shown). Moreover, in a parallel study in MPS I mice (unpublished data), when a 10 fold-dose of this gene editing system used, no vector-associated toxicity or microscopic findings were observed in the 11-month follow-up. These results further support the feasibility of increasing the dose to improve the efficacy.

ACKNOWLEDGEMENTS

8. REFERENCES

[1]. Ou L, Przybilla MJ, Whitley CB. SAAMP 2.0: an algorithm to predict genotype-phenotype correlation of lysosomal storage diseases. Clin Genet. 2018;93(5):1008–14. [PubMed: 29396849]

[2]. Ou L, Przybilla MJ, Whitley CB. Phenotype prediction for mucopolysaccharidosis type I by in silico analysis. Orphan J Rare Dis. 2017;12(1):125.

[3]. Ou L, Kim S, Whitley CB, Jarnes-Utz JR. Genotype-phenotype correlation of gangliosidosis mutations using in silico tools and homology modeling. Mol Genet Metab Rep. 2019;20:100495. [PubMed: 31367523]

[4]. Jarnes Utz JR, Kim S, King K, Ziegler R, Schema L, Redtree ES, et al. Infantile gangliosidoses: Mapping a timeline of clinical changes. Mol Genet Metab. 2017;121(2):170–9. [PubMed: 28476546]

[5]. Whitley CB, Anderson RA, McIvor RS. Heterozygosity for the DN allele (G533>A) of the β-hexosaminidase α subunit gene identified by direct DNA sequencing in a family with the B1 variant of GM2-gangliosidosis. Neuropediatrics. 1992;23(2):96–101. [PubMed: 1318511]

[6]. Karumuthil-Melethil S, Nagabhushan Kalburgi S, Thompson P, Tropak M, Kaytor MD, Keimel JG, et al. Novel vector design and hexosaminidase variant enabling self-complementary adeno-associated virus for the treatment of Tay-Sachs disease. Hum Gene Ther. 2016;27(7):509–21. [PubMed: 27197548]

[7]. Osmon KJ, Woodley E, Thompson P, Ong K, Karumuthil-Melethil S, Keimel JG,et al. Systemic gene transfer of a hexosaminidase variant using an scAAV9.47 vector corrects GM2 gangliosidosis in Sandhoff mice. Hum Gene Ther. 2016;27(7):497–508. [PubMed: 27199088]

[8]. Bradbury AM, Cochran JN, McCurdy VJ, Johnson AK, Brunson BL, Gray-Edwards H, et al. Therapeutic response in feline Sandhoff disease despite immunity to intracranial gene therapy. Mol Ther. 2013;21(7):1306–15. [PubMed: 23689599]

[9]. Ou L, DeKelver R, Rhode M, Tom S, Radeke R, St Martin SJ, et al. ZFN-Mediated In Vivo Genome Editing Corrects Murine Hurler Syndrome. Mol Ther. 2019;27(1):178–87. [PubMed: 30528089]

[10]. Harmatz P, Lau HA, Helderman C, Leslie N, Foo CWP, Vaidya SA, et al. EMPOWERS: A phase 1/2 clinical trial of SB-318 ZFN-mediated in vivo human genome editing for treatment of MPS I (Hurler syndrome). Mol Genet Metab. 2019; 126(2):S68 (abstract 147).

[11]. Tropak MB, Yonekawa S, Karumuthil-Melethil S, Thompson P, Wakarchuk W, Gray SJ, et al. Construction of a hybrid β-hexosaminidase subunit capable of forming stable homodimers that hydrolyze GM2 ganglioside in vivo. Mol Ther Methods Clin Dev. 2016;3:15057. [PubMed: 26966698]

[12]. Sango K, Yamanaka S, Hoffmann A, Okuda Y, Grinberg A, Westphal H, et al. Mouse models of Tay-Sachs and Sandhoff diseases differ in neurologic phenotype and ganglioside metabolism. Nat Genet. 1995;11(2):170–6. [PubMed: 7550345]

[13]. Aronovich EL, Hall BC, Bell JB, McIvor RS, Hackett PB. Quantitative analysis of α-L-iduronidase expression in immunocompetent mice treated with the Sleeping Beauty transposon system. PLoS One. 2013;8(10):e78161. [PubMed: 24205141]

[14]. Wang D, El-Amouri SS, Dai M, Kuan CY, Hui DY, Brady RO, et al. Engineering a lysosomal enzyme with a derivative of receptor-binding domain of apoE enables delivery across the blood-brain barrier. Proc Natl Acad Sci USA. 2013;110(8):2999–3004. [PubMed: 23382178]

[15]. Ou L, Przybilla MJ, Koniar BL, Whitley CB. Elements of lentiviral vector design study toward gene therapy for treating mucopolysaccharidosis I. Mol Genet Metab Rep. 2016; 8:93–97.

[16]. Przybilla MJ, Ou L, T b ran A, Jiang X, Sidhu R, Kell PJ, et al. Comprehensive behavioral and biochemical outcomes of novel murine models of GM1-gangliosidosis and Morquio syndrome type B. Mol Genet Metab. 2019;126(2):139–50. [PubMed: 30528226]

[17]. Ogawa N, Hirose Y, Ohara S, Ono T, Watanabe Y. A simple quantitative bradykinesia test in MPTP-treated mice. Res Commun Chem Pathol Pharmacol 1985;50(3):435–41. [PubMed: 3878557]

[18]. Hockly E, Woodman B, Mahal A, Lewis CM, Bates G. Standardization and statistical approaches to therapeutic trials in the R6/2 mouse. Brain Res Bull. 2003;61(5):469–79. [PubMed: 13679245]

[19]. Martin-Fernandez M, Jamison S, Robin LM, Zhao Z, Martin ED, Aguilar J, et al. Synapse-specific astrocyte gating of amygdala-related behavior. Nat Neurosci. 2017;20(11):1540–8. [PubMed: 28945222]

[20]. Sands MS, Davidson BL. Gene therapy for lysosomal storage diseases. Mol Ther. 2006;13(5):839–49. [PubMed: 16545619]

[21]. Ou L, Herzog T, Koniar BL, Gunther R, Whitley CB. High-dose enzyme replacement therapy in murine Hurler syndrome. Mol Genet Metab. 2014;111(2):116–22. [PubMed: 24100243]

[22]. Cho SY, Lee J, Ko AR, Kwak MJ, Kim S, Sohn YB, et al. Effect of systemic high dose enzyme replacement therapy on the improvement of CNS defects in a mouse model of mucopolysaccharidosis type II. Orphanet J Rare Dis. 2015;10:141. [PubMed: 26520066]

[23]. Rozaklis T, Beard H, Hassiotis S, Garcia AR, Tonini M, Luck A, et al. Impact of high-dose, chemically modified sulfamidase on pathology in a murine model of MPS IIIA. Exp Neurol. 2011;230(1):123–30. [PubMed: 21515264]

[24]. Vogler C, Levy B, Grubb JH, Galvin N, Tan Y, Kakkis E, et al. Overcoming the blood-brain barrier with high-dose enzyme replacement therapy in murine mucopolysaccharidosis VII. Proc Natl Acad Sci USA. 2005;102(41):14777–82. [PubMed: 16162667]

[25]. Lee WC, Courtenay A, Troendle FJ, Stallings-Mann ML, Dickey CA, DeLucia MW, et al. Enzyme replacement therapy results in substantial improvements in early clinical phenotype in a

mouse model of globoid cell leukodystrophy. FASEB J. 2005;19(11):1549–51. [PubMed: 15987783]

[26]. Matzner U, Herbst E, Hedayati KK, Lüllmann-Rauch R, Wessig C, Schröder S, et al. Enzyme replacement improves nervous system pathology and function in a mouse model for metachromatic leukodystrophy. Hum Mol Genet. 2005;14(9):1139–52. [PubMed: 15772092]

[27]. Blanz J, Stroobants S, Lüllmann-Rauch R, Morelle W, Lüdemann M, D'Hooge R, et al. Reversal of peripheral and central neural storage and ataxia after recombinant enzyme replacement therapy in alpha-mannosidosis mice. Hum Mol Genet. 2008;17(22):3437–45. [PubMed: 18713755]

[28]. Dunder U, Kaartinen V, Valtonen P, Väänänen E, Kosma VM, Heisterkamp N, et al. Enzyme replacement therapy in a mouse model of aspartylglycosaminuria. FASEB J. 2000;14(2):361–7. [PubMed: 10657992]

[29]. Laoharawee K, DeKelver RC, Podetz-Pedersen KM, Rohde M, Sproul S, Nguyen HO, et al. Dose-dependent prevention of metabolic and neurologic disease in murine MPS II by ZFN-mediated in vivo genome editing. Mol Ther. 2018;26(4):1127–1136. [PubMed: 29580682]

[30]. Hu L, Sun Y, Villasana LE, Paylor R, Klann E, Pautler RG. Early changes in the apparent diffusion coefficient (ADC) in a mouse model of Sandhoff's disease occur prior to disease symptoms and behavioral deficits. Magn Reson Med. 2009 11;62(5):1175–84. [PubMed: 19780154]

[31]. Aschauer DF, Kreuz S, Rumpel S. Analysis of transduction efficiency, tropism and axonal transport of AAV serotypes 1, 2, 5, 6, 8 and 9 in the mouse brain. PLoS One. 2013;8(9):e76310. [PubMed: 24086725]

[32]. Itakura T, Kuroki A, Ishibashi Y, Tsuji D, Kawashita E, Higashine Y, et al. Inefficiency in GM2 ganglioside elimination by human lysosomal beta-hexosaminidase beta-subunit gene transfer to fibroblastic cell line derived from Sandhoff disease model mice. Biol Pharm Bull. 2006;29(8):1564–9. [PubMed: 16880605]

[33]. Cachón-González MB, Wang SZ, Lynch A, Ziegler R, Cheng SH, Cox TM. Effective gene therapy in an authentic model of Tay-Sachs-related diseases. Proc Natl Acad Sci USA. 2006;103(27):10373–8. [PubMed: 16801539]

[34]. Kytzia HJ, Sandhoff K. Evidence for two different active sites on human beta-hexosaminidase A. Interaction of GM2 activator protein with beta-hexosaminidase A. J Biol Chem. 1985 6 25;260(12):7568–72. [PubMed: 3158659]

[35]. Tsuji D, Akeboshi H, Matsuoka K, Yasuoka H, Miyasaki E, Kasahara Y, et al. Highly phosphomannosylated enzyme replacement therapy for GM2 gangliosidosis. Ann Neurol. 2011;69(4):691–701. [PubMed: 21520232]

[36]. Maegawa GH, Banwell BL, Blaser S, Sorge G, Toplak M, Ackerley C, et al. Substrate reduction therapy in juvenile GM2 gangliosidosis. Mol Genet Metab. 2009;98(1–2):215–24. [PubMed: 19595619]

[37]. Osher E, Fattal-Valevski A, Sagie L, Urshanski N, Amir-Levi Y, Katzburg S, et al. Pyrimethamine increases β-hexosaminidase A activity in patients with Late Onset Tay Sachs. Mol Genet Metab. 2011;102(3):356–63. [PubMed: 21185210]

[38]. Jacobs J, Willemsen M, Groot-Loonen J, Wevers RA, Hoogerbrugge PM. Allogeneic BMT followed by substrate reduction therapy in a child with subacute Tay-Sachs disease. Bone Marrow Transplant. 2005;36(10):925–6. [PubMed: 16151419]

[39]. Kyrkanides S, Miller JH, Brouxhon SM, Olschowka JA, Federoff HJ. beta-hexosaminidase lentiviral vectors: transfer into the CNS via systemic administration. Brain Res Mol Brain Res. 2005;133(2):286–98. [PubMed: 15710246]

[40]. Cachón-González MB, Wang SZ, McNair R, Bradley J, Lunn D, Ziegler R, et al. Gene transfer corrects acute GM2 gangliosidosis--potential therapeutic contribution of perivascular enzyme flow. Mol Ther. 2012;20(8):1489–500. [PubMed: 22453766]

[41]. Hacein-Bey-Abina S, Von Kalle C, Schmidt M, McCormack MP, Wulffraat N, Leboulch P, et al. LMO2-associated clonal T cell proliferation in two patients after gene therapy for SCID-X1. Science. 2003;302(5644):415–9. [PubMed: 14564000]

[42]. Nakai H, Yant SR, Storm TA, Fuess S, Meuse L, Kay MA. Extrachromosomal recombinant adeno-associated virus vector genomes are primarily responsible for stable liver transduction in vivo. J Virol. 2001;75(15):6969–76. [PubMed: 11435577]

[43]. Calcedo R, Wilson JM. Humoral Immune Response to AAV. Front Immunol. 2013;4:341. [PubMed: 24151496]

[44]. Walia JS, Altaleb N, Bello A, Kruck C, LaFave MC, Varshney GK, et al. Long-term correction of Sandhoff disease following intravenous delivery of rAAV9 to mouse neonates. Mol Ther. 2015;23(3):414–22. [PubMed: 25515709]

[45]. Maeder ML, Stefanidakis M, Wilson CJ, Baral R, Barrera LA, Bounoutas GS, et al. Development of a gene-editing approach to restore vision loss in Leber congenital amaurosis type 10. Nat Med. 2019;25(2):229–33. [PubMed: 30664785]

[46]. Zuo E, Sun Y, Wei W, Yuan T, Ying W, Sun H, et al. Cytosine base editor generates substantial off-target single-nucleotide variants in mouse embryos. Science. 2019;364(6437):289–92. [PubMed: 30819928]

[47]. Ou L, Przybilla MJ, Whitley CB. Metabolomics profiling reveals profound metabolic impairments in mice and patients with Sandhoff disease. Mol Genet Metab. 2019;126(2):151–6. [PubMed: 30236619]

[48]. Passini MA, Lee EB, Heuer GG, Wolfe JH. Distribution of a lysosomal enzyme in the adult brain by axonal transport and by cells of the rostral migratory stream. J Neurosci. 2002;22(15):6437–46. [PubMed: 12151523]

[49]. Golebiowski D, van der Bom IM, Kwon CS, Miller AD, Petrosky K, Bradbury AM, et al. Direct intracranial injection of AAVrh8 encoding monkey β-N-acetylhexosaminidase causes neurotoxicity in primate brain. Hum Gene Ther. 2017;28(6):510–22. [PubMed: 28132521]

[50]. Dogbevia G, Grasshoff H, Othman A, Penno A, Schwaninger M. Brain endothelial specific gene therapy improves experimental Sandhoff disease. J Cereb Blood Flow Metab. 2019 7 29:271678X19865917.

[51]. Ou L, Przybilla MJ, Koniar B, Whitley CB. RTB lectin-mediated delivery of lysosomal α-l-iduronidase mitigates disease manifestations systemically including the central nervous system. Mol Genet Metab. 2018;123(2):105–11. [PubMed: 29198892]

A

B

gRNA	indels%
mALB-g1	11%
mALB-g2	2%
mALB-g3	0
mALB-g4	0

C
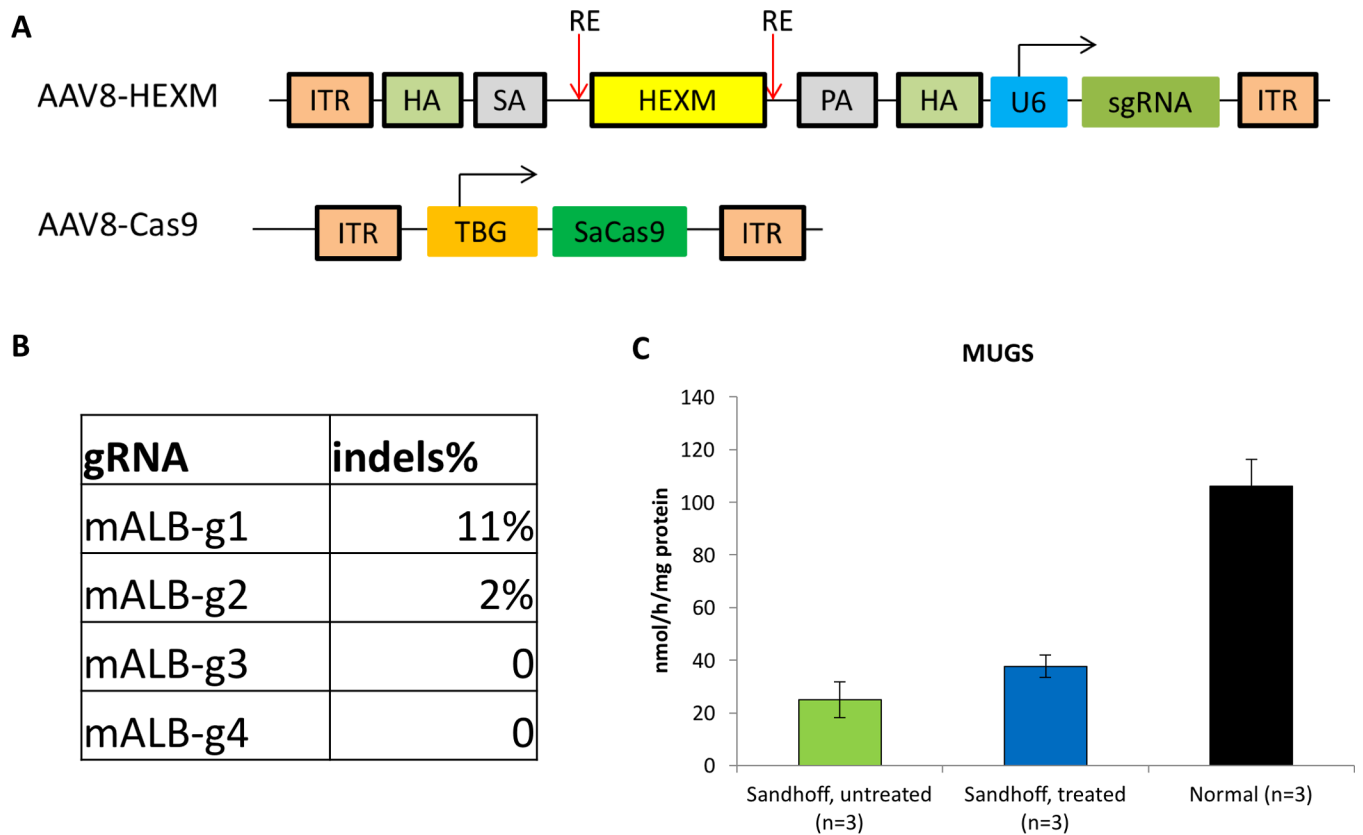
**Fig. 1. Construct design and gRNA validation by Surveyor assay.**
(**A**) Sequence of AAV vectors represented in cartoon. TBG: thyroxine-binding globulin; ITR: inverted terminal repeats; SA: splicing acceptor; PA: polyA; ITR: inverted terminal repeat; HA: homology arm; HEXM: cDNA of the μ subunit; RE: restriction enzyme site; U6: U6 promoter. (**B**) Surveyor assay for gRNA activity in MEF cells. Each gRNA construct was transfected into MEF cells, and subsequently harvested for PCR amplification. In order to determine the gRNA cleavage activity of the gRNA constructs, an *in vitro* Surveyor assay was performed on the PCR products. (**C**) MUG activities in the liver increased significantly 2 days after hydrodynamic injection of AAV-SaCas9 and AAV-HEXB-gRNA plasmids into Sandhoff mice (n=3). * p<0.05 when comparing treated Sandhoff mice to untreated Sandhoff mice.
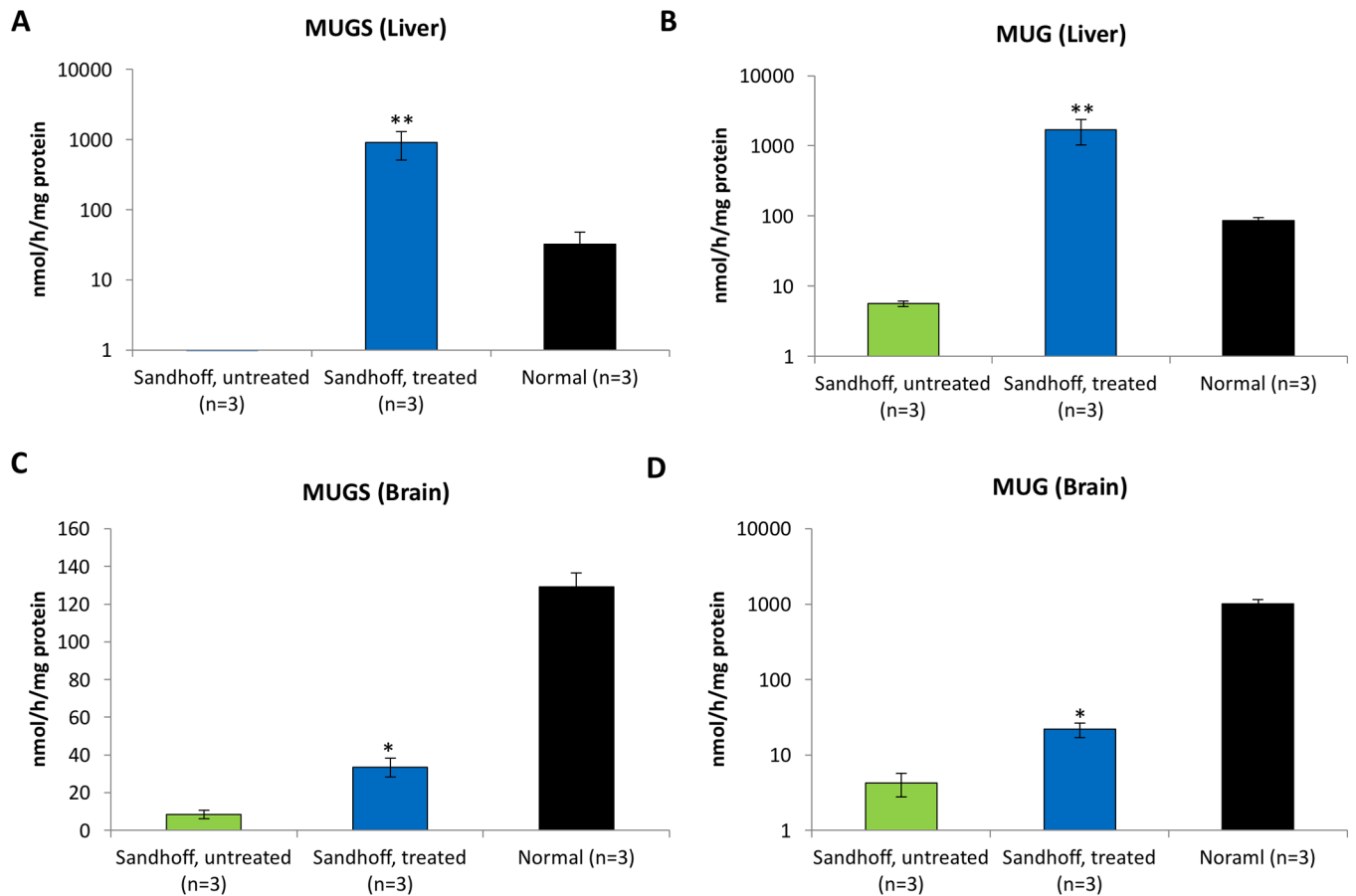
Fig. 2. Hydrodynamic injection of plasmids encoding HEXM sequence into adult Sandhoff mice.
MUGS and MUG activities in the liver and brain of treated mice increased significantly 2 days post-dosing. * p<0.05 when comparing treated Sandhoff mice to untreated Sandhoff mice.
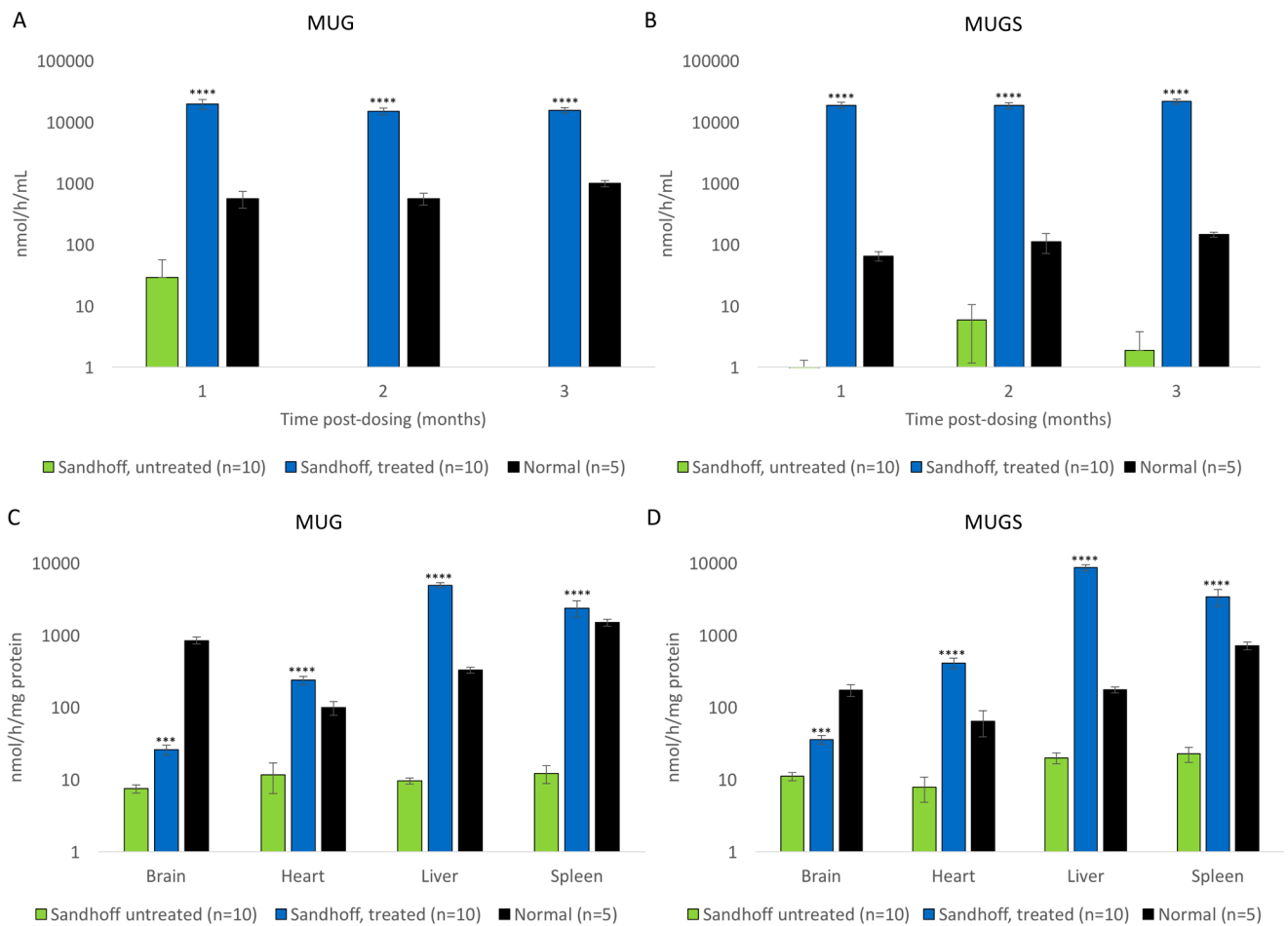
Fig. 3. Plasma and tissue Hex enzyme activities increased significantly after AAV injection.
Plasma MUGS (**A**) and MUG (**B**) activities significantly increased on Day 30, 60 and 90 post dosing. Four months post dosing, all mice were euthanized after transcardial perfusion. The brain, liver, heart and spleen were harvested for enzyme assays. Tissue MUGS (**C**) and MUG (**D**) activities increased significantly. *** p<0.001 when comparing treated Sandhoff mice to untreated Sandhoff mice, **** p<0.0001.
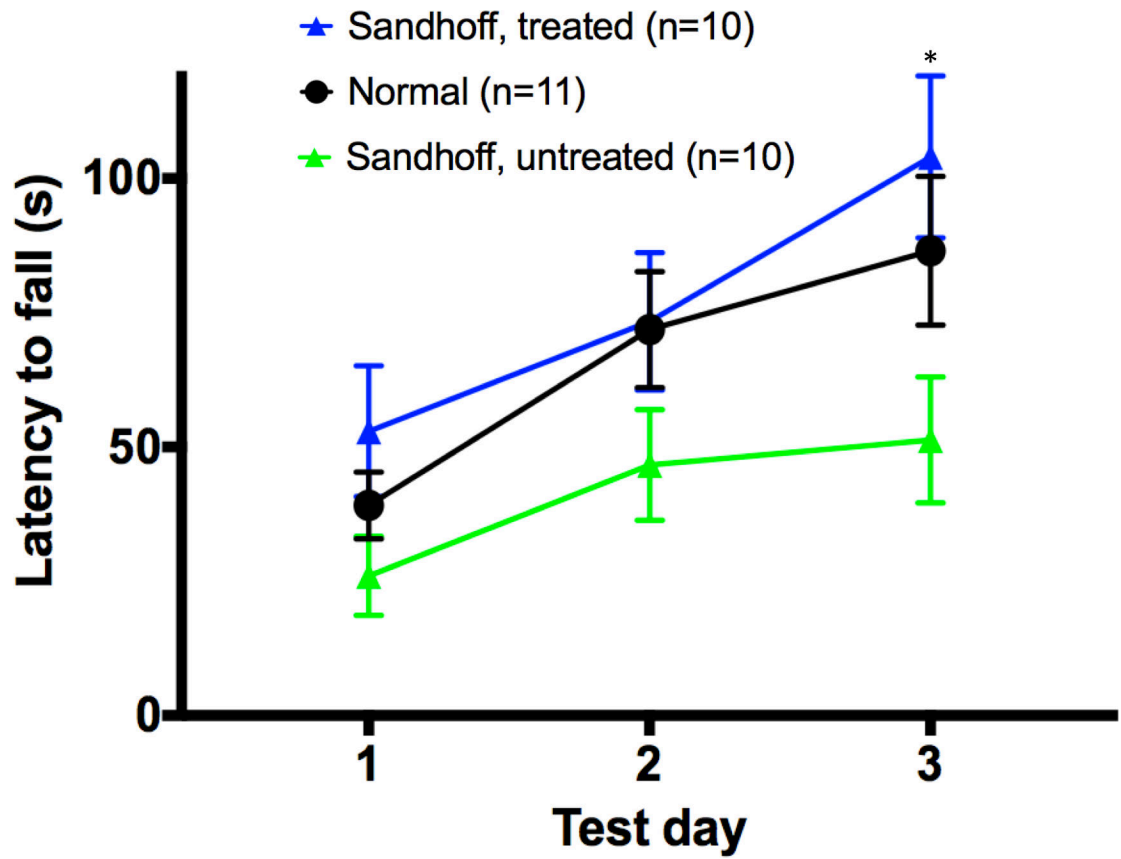
Fig. 4. Rotarod analysis showed that treated Sandhoff mice had significant improved performance.

* p<0.05 when comparing treated Sandhoff mice to untreated Sandhoff mice.
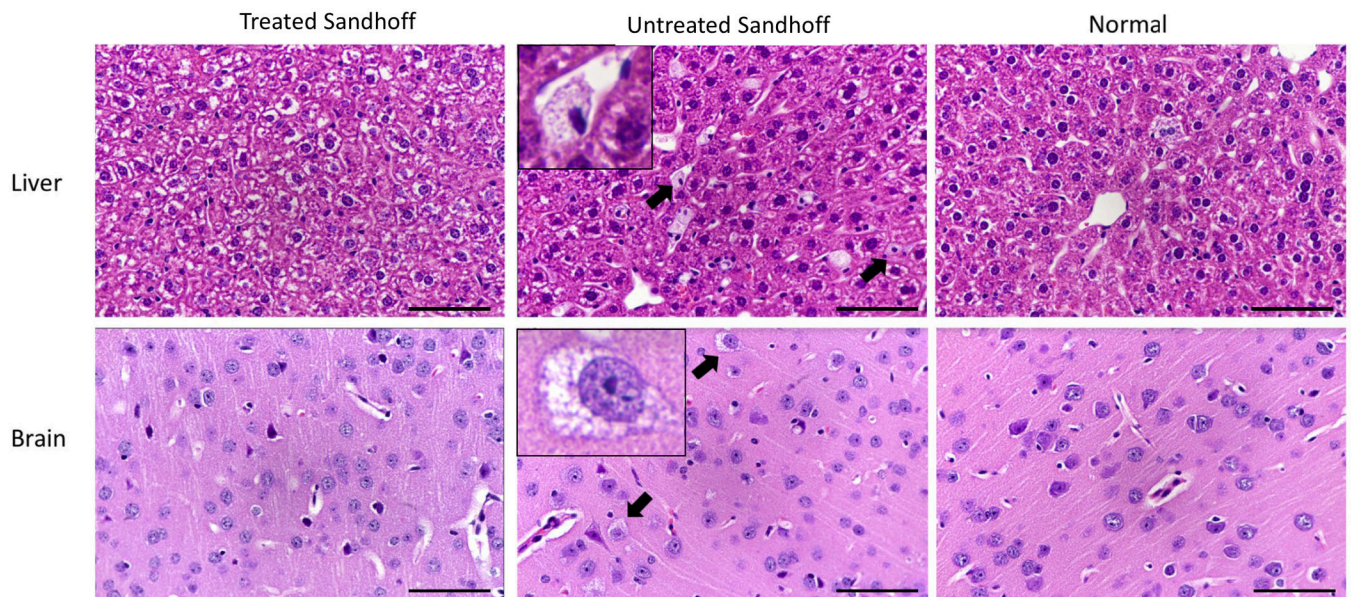
Fig. 5. Histological analysis showed that cellular vacuolation was reduced in the brain and liver of treated Sandhoff mice.

The brain (upper panel) and liver (lower panel) were processed for H&E staining. Treated Sandhoff mice, untreated Sandhoff and normal mice are shown in the left, middle and right columns, respectively. Kupffer cell vacuolation (small, well defined, vesicles with clear to pale-eosinophilic content) in the liver of untreated Sandhoff mice was reduced in treated Sandhoff mice. In the cerebellum, pons, thalamus, hypothalamus and brain cortex of untreated Sandhoff mice, there was neuronal vacuolation, which was significantly reduced in 1 of 3 treated Sandhoff and was not observed in normal mice. Objective x40.
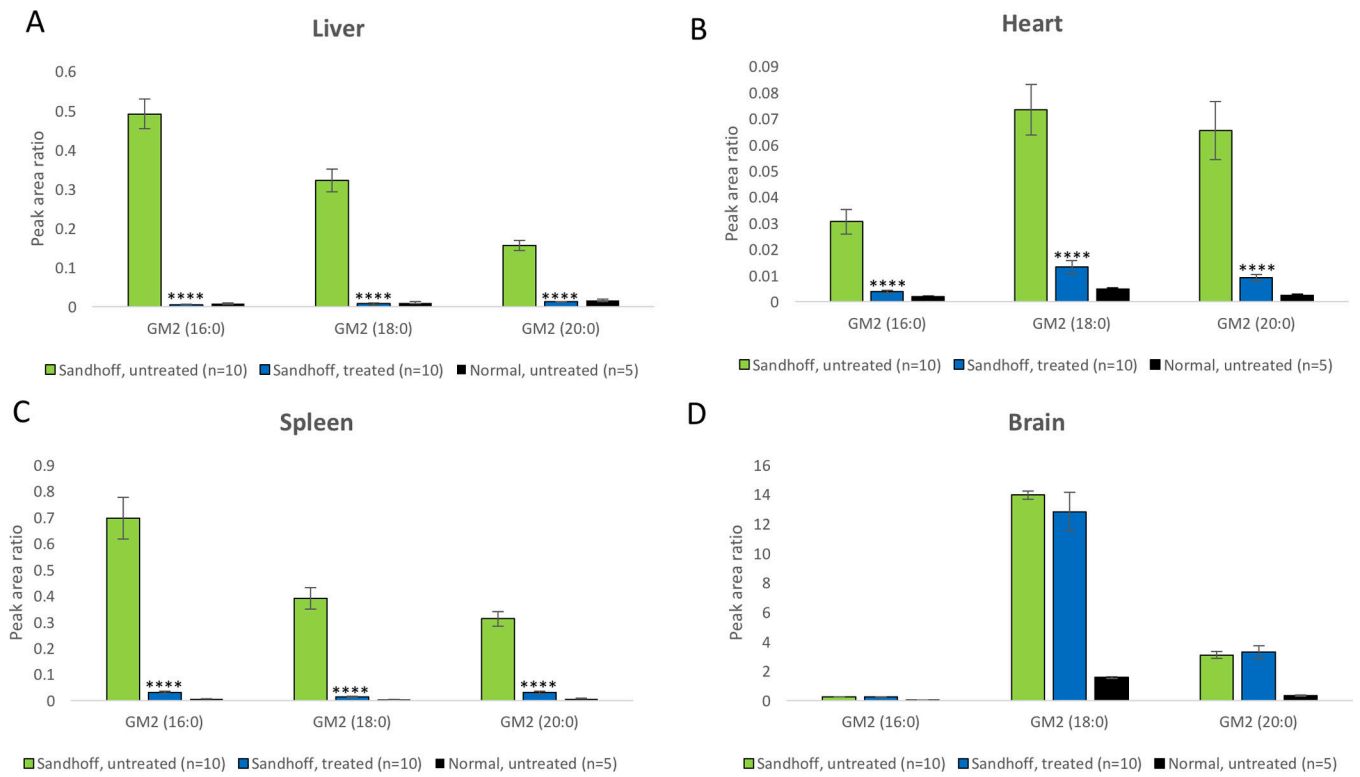
Fig. 6. Tissue GM2 gangliosides reduced 4 months post dosing.
GM2 gangliosides in the liver (**A**), heart (**B**), spleen (**C**) and brain (**D**) were quantified by HPLC-MS/MS. **** $p<0.0001$ when comparing treated Sandhoff mice to untreated Sandhoff mice.

Table 1:

Previous preclinical studies show that high doses of ERT can treat neurological complications.

Mouse model	Dose (mg/kg)	Clinical dose (mg/kg)	Brain enzyme activity (% Normal)	Brain storage reduced (%Affected)	References
α-mannosidosis	36.6	1	15%	50%	[27]
Metachromatic leukodystrophy	20	N/A	N/A	30%	[26]
Aspartylglycosaminuria	10	N/A	10%	20%	[28]
Krabbe disease	6	N/A	7%	18%	[25]
MPS II	10	0.5	5%	N/A	[22]
MPS IIIA	20	N/A	22%	0	[23]
MPS VII	20	2	2.50%	N/A	[24]
MPS I	20	0.58	97%	63%	[21]

Table 2.

AAV copy number in tissues.

Group assignment	AAV copy number (100vg/ng DNA)			
	Brain	**Liver**	**Heart**	**Spleen**
Normal (n=4)	ND	ND	ND	ND
Sandhoff, untreated (n=4)	ND	ND	ND	ND
Sandhoff, treated (n=6)	11.1±4.1	2,155±661	1,461±385	ND

ND, non-detectable.